Heat flow estimates offshore Haiti in the Caribbean plate

Frédérique Rolandone, Francis Lucazeau, Jeffrey Poort, Sylvie Leroy

DR FRÉDÉRIQUE ROLANDONE (Orcid ID : 0000-0001-5339-4275)

DR FRANCIS LUCAZEAU (Orcid ID : 0000-0003-2481-1222)

DR SYLVIE LEROY (Orcid ID : 0000-0002-3188-8802)

Article type : Research Article

Corresponding Author Email ID: frederique.rolandone@upmc.fr

Heat-flow estimates offshore Haiti in the Caribbean plate

Frédérique Rolandone[1], Francis Lucazeau[2], Jeffrey Poort[1], Sylvie Leroy[1]

[1]Sorbonne Université, CNRS-INSU, Institut des Sciences de la Terre Paris, ISTeP UMR 7193, F-75005 Paris, France.

[2]Université de Paris, Institut de physique du globe de Paris, CNRS, F-75005 Paris, France

Abstract

Heat-flow in the Caribbean is poorly known and generally low in the major basins and the Greater Antilles arc, but with some high values in active zones, like in the Cayman trough or in the Lesser Antilles Arc. Here we present new heat-flow data for offshore Haiti, which is part of the Greater Antilles arc. We obtain new heat-flow estimates from in situ measurements and

This article has been accepted for publication and undergone full peer review but has not been through the copyediting, typesetting, pagination and proofreading process, which may lead to differences between this version and the Version of Record. Please cite this article as doi: 10.1111/ter.12454

Bottom Simulating Reflector (BSR). Both methods suggest a regionally low heat-flow, respectively 46±7 mWm^{-2} and 44±12 mWm^{-2}, with locally high values exceeding 80 mWm^{-2}. The high heat-flow values are generally located near faults, and could be related to fluid circulations. Our study confirms a low heat-flow pattern at the scale of the Caribbean but points out the existence of local-scale variability with high heat-flow along the northern faults of the Caribbean region.

1. Introduction

The structure and evolution of the Caribbean region result from the tectonic interactions of several major plates through time. The Caribbean plate formed in the Pacific during the Jurassic and thickened in the Cretaceous above a mantle plume/hotspot, that led to a large igneous province, the Caribbean Large Igneous Province (CLIP) (Loewen et al., 2013). The morphology of the oceanic domain of the Caribbean is governed by basins and structural highs, from west to east: the Yucatan Basin, the Cayman Trough, the Nicaraguan Rise, the Colombian Basin, the Beata Ridge, the Venezuelan Basin, the Aves Ridge and the Grenada Basin (Mauffret and Leroy, 1997). The Caribbean oceanic domain is bounded by the Lesser Antilles arc to the east and the Greater Antilles arc (Cuba, Hispaniola, Puerto Rico) to the north (Fig. 1). The Caribbean plate is moving eastward from North America, resulting in a 3000 km long and 200 km wide deformation zone, the Northern Caribbean plate boundary (Mann et al., 1991; Calais et al., 1998, 2016). A significant seismic activity is associated with this deformation, notably along two large strike-slip faults, the Septentrional–Oriente fault zone (SOFZ) in the north and the Enriquillo–Plantain-Garden fault zone (EPGFZ) in the south (Fig. 1).

The surface heat-flow in the Caribbean plate is poorly known, with mostly old and scarce marine measurements. From previous measurements (Fig. 1), heat-flow is regionally low: 46±23 mWm^{-2} (based on N=15 data) in the Yucatan basin (Epp et al., 1970; Erickson et al., 1972; Khutorskoy et al., 1990), 60±19 mWm^{-2} (N=24) in the Colombian basin (Epp et al., 1970; Langseth et al., 1971; Bookman et al., 1972), 56±11 mWm^{-2} in the Beata ridge (Epp et al., 1970) and 50±16 mWm^{-2} (N=20) in the Venezuelan basin (Epp et al., 1970; Bookman et al., 1973). High heat-flow 83 ± 17 mWm^{-2} is observed in the Cayman trough (N=10) (Erickson et al., 1972; Rosencrantz et

al., 1988). Other high values 139±63 mWm^{-2} are observed in the Aves ridge, the Grenada Basin and the active Lesser Antilles volcanic arc (Clark et al., 1978; Vacquier and von Herzen, 1964; Nason and Lee, 1964; Epp et al., 1970; Manga et al., 2012). In the terrestrial domains, heat-flow determined in Cuba and Puerto Rico is also low. In Cuba, Cermak et al. (1984, 1991) estimate the average heat-flow to 47±14 mWm^{-2} (N=35). In Puerto Rico, Anderson and Larue (1991) estimate an average heat-flow of 30-50 mWm^{-2}.

In the region around Haiti, the western part of Hispaniola, no heat-flow measurements existed before the marine geophysical and geological survey HAITI-SIS (Leroy et al., 2015; Corbeau et al., 2016a,b). The main objective of HAITI-SIS was to study the past and present deformation of the North America-Caribbean plate boundary using highresolution multi-beam echo sounder and shallow seismic reflection profiles. During HAITISIS, we equipped the Küllenberg piston cores with thermal sensors and obtained 12 new heat-flow estimates. In addition, heat-flow was derived from observations of the Bottom Simulating Reflector (BSR) along 7 seismic profiles acquired during HAITI-SIS.

2. Results

Heat-flow density represents the Earth heat loss on a surface unit, and is obtained as the product of the vertical temperature gradient by the thermal conductivity of rocks. We estimate heat-flow in two ways: (1) from autonomous thermal probes attached to a Küllenberg piston core and (2) from the depth of the BSR, identified them on seismic profiles (see Supplementary Material).

2.1. Heat-flow from cores

We measured the temperature gradient and thermal conductivity on twelve cores (Tables 1 and 2; Fig. 2). KT01 is the only measurement south of EPGFZ (Fig. 1) and the estimated heat-flow is 85.0±15.0 mWm^{-2}. Three measurements (KT04-05-06) were obtained in the Jeremie Basin (Fig. 3). The average heat-flow is low, 45.5±3.2 mWm^{-2}. Three other measurements (KT07-08-10) obtained in the Gonave Basin provide a similar heat-flow, 40.5±5.0 mWm^{-2}. KT12 is the only core located north of SOFZ. The heat-flow is relatively high, 89.0±5.9 mWm^{-2}, similar to the value

observed at KT01. KT13 is located close to SOFZ. The average temperature gradient is high, a minimum of 163 mKm^{-1} is obtained (377 mWm^{-2} for the lower two points). Heat-flow is consequently very high: 177.0±21.1 mWm^{-2}. The last three measurements (KT14-15-16), obtained in the Artibonite Basin, have more variable thermal characteristics and heat-flow, 75.2±15.3 mWm^{-2}, is higher than in the Jeremie and Gonave Basins.

2.2. Heat-flow from BSR

BSR are observed along seismic profiles in the Artibonite basin (Fig. 3). The average of 2489 values, 43.7±12.4 mW m^{-2}, is similar to values observed in the Jeremie and Gonave Basins. High heat-flow values are found along the profiles H12-118 (100-110 mWm^{-2}, Fig. 4) and H12-103 (60-80 mWm^{-2}, Fig. 5). Comparison of heat-flow estimated from the measured temperature gradient and conductivity with heat-flow derived from the depth of BSR can be done at site KT16. At the closest shot (H12-118-1727), the estimated heat-flow is 82.8±20.4 mWm^{-2}, whereas heat-flow at site KT16 is 77.1±6.4 mWm^{-2}. The transition from low to high heat-flow near site KT16 occurs abruptly. This is characteristic of a superficial cause (Hutnak et al., 2007), and observed in the vicinity of a reverse fault (Corbeau et al., 2016b) and of a basement relief (Fig. 3). On profile H12-103, higher heat-flow is also observed close to a mapped fault. However, the other reverse faults crossing the profiles have no effect on heat-flow.

3. Discussion

3.1 Heat-flow offshore Haiti

The heat-flow estimates from the Haiti region have an average of respectively 46±7 mWm^{-2} and 44±12 mWm^{-2} for sediment cores and BSR. Similar heat-flow (40-50 mWm^{-2}) is derived from 3 exploration drill-holes (see Supplementary Material, Fig. 3). Background heat-flow can thus be considered as low as in the surrounding regions. High values are only found near the large strike-slip faults system (SOFZ and EPGFZ) or near smaller reverse faults (Figs. 1-3). Because they are spatially localized, these anomalies are necessarily superficial but could have several possible

causes.

Heat generated by frictional or viscous shear heating on active faults such as EPGFZ and SOFZ is a possible mechanism with theoretical support (Brune et al. 1969; Mase and Smith, 1987; Rolandone and Jaupart, 2002). However, the effect on surface heat-flow was never evidenced on large fault systems such as San Andreas with thermal anomalies less than 20 mWm^{-2} (Brune et al., 1969; Lachenbruch and Sass, 1992). For smaller faults observed west of Haiti, this effect is even more unlikely.

Heat refraction caused by thermal conductivity contrasts and/or sea-bottom topography is another possible mechanism leading to localized anomalies. Erickson et al. (1972) questioned a similar observation in Cayman trough and showed that the most important perturbation at crustal scale is caused by the irregularities of the sea floor, with a maximum of about 10-20% of the background heat-flow value. For Haiti, the topographic effect is however negligible and no large conductivity contrast is expected from the local geology.

None of these conductive mechanisms can thus explain heat-flow values as high as 100-180 mWm^{-2} for a background heat-flow of 45 mWm^{-2}. Alternatively, hydrothermal circulation is known as an efficient mechanism in oceanic domain (Fisher and Wheat, 2010). Hydrothermal circulation has been observed at the ridge axis and also on their flanks (Le Gal et al., 2018). Deep (4960 m) and hot (401 °C) hydrothermal circulations were identified in the Cayman trough (Webber et al., 2015, 2017). Large faults, such as the SOFZ and EPGFZ, could be a pathway for hydrothermal circulation. However, fluid circulation as a source for the high heat-flow anomaly observed near faults is still a speculative interpretation. The relationship between active faults and fluids is not well understood and. no other observations for fluid flow have been reported for our marine study area. It would require more data to characterize the possible hydrothermal system.

3.2 Heat-flow in the Caribbean

The Caribbean plate is characterized by Jurassic or Early Cretaceous oceanic crust overlain by Upper Cretaceous plateau basalts (CLIP) with different thicknesses (Fig. 6a, Mauffret and Leroy,

1997). In the Yucatan basin, the Colombian basin, the Beata ridge and the Venezuelan basin, the average heat-flow is low 40-60 mWm^{-2} (Epp et al., 1970; Erickson et al., 1972; Khutorskoy et al., 1990; Langseth et al., 1971; Bookman et al., 1972, 1973). Oceanic crust in the Cayman Trough is of different age from the CLIP domain and results from post-49 Ma ultra-slow spreading (Leroy et al 2000; Hayman et al., 2011). High heat-flow around 100 mWm^{-2} observed in the Cayman trough was first attributed to crustal extension and a typical cooling evolution (Erickson et al., 1972), but highest values cannot be explained by this process and are rather associated with major strike-slip faults (Rosencrantz et al., 1988) and with hydrothermal circulations (Webber et al., 2015, 2017).

The Caribbean plate is also characterized by two island arcs, the Greater (Cuba, Hispaniola, Puerto Rico) and Lesser Antilles arcs initiated during Cretaceous. These arcs are composed of volcanic island-arc related plutonic and extrusive rocks (Fig. 6a). Present day island-arc volcanism is limited to the Lesser Antilles arc. High heat-flow is observed in the Aves ridge, the Grenada Basin and the active Lesser Antilles volcanic arc (Clark et al., 1978; Vacquier and von Herzen, 1964; Nason and Lee, 1964; Epp et al., 1970; Manga et al., 2012). High heat-flow is associated to the volcanic arc, up to 250 mWm^{-2} (Clark et al., 1978) or up to 100 mWm^{-2} (Manga et al., 2012). The Grenada basin is an Eocene back-arc basin with heat-flow values in the range 50-90 mWm^{-2}. High heat-flow values 100-240 mWm^{-2} were found in the Aves ridge (Clark et al., 1978), a remnant early Paleogene arc, formerly active island arc (Neill et al., 2011). These high values, based on very shallow measurements, were questioned by Manga et al. (2012). Once excluded, Manga et al. (2012) argue that there is no longer a clear distinction between the Aves ridge and the Grenada basin. In the predictive heat-flow map (Fig. 6b), we do not use the high heat-flow values of Clark et al. (1978). The heat-flow measurements of the Lesser Antilles are characteristic of the distribution of heat-flow across ocean island arc with hot arc and back-arc.

Along the Greater Antilles arc, arc magmatism was only active until early to middle Eocene in eastern Cuba and Hispaniola and middle Eocene in Puerto Rico (Lidiak and Jolly, 1996). In Cuba and Puerto Rico, the average heat-flow is low, 30-50 mWm^{-2} (Cermak et al., 1984, 1991; Anderson and Larue, 1991). Our measurements offshore Haiti confirm a regionally low heat-flow. Lewis et al. (2011) and Rojas-Agramonte et al. (2004) provide

geochemical data showing that Caribbean granites have a very low radiogenic content. The Terre-Neuve granite in Haiti has a resulting heat production of only 0.9 μWm^{-3}. Granitoids of the Greater Antilles arc (e.g. Terre-Neuve in Haiti, Above-Rocks in Jamaica, Sierra-Maestra in Cuba) have all a low radiogenic contribution of the crust to the surface heat-flow. If the northern part of Haiti has a crust composed of island-arc facies, the southern part of Haiti has a typical geochemical signature of CLIP (Loewen et al., 2013, Fig.6a). A receiver function study (Corbeau et al., 2017) suggests that the crustal domain north of EPGFZ in Haiti is underlain by about 10 km of CLIP material, and thus that a large part of the crust in Haiti is made of underplated and low radiogenic basaltic material. A tomographic study (Possee et al., 2019) also indicates that southern and central Haiti are characterized by a dominantly mafic composition of the crust and thus a low radiogenic heat contribution to the heat-flow.

The regional heat-flow pattern of the Caribbean is well expressed by a heat-flow map based on the heat-flow measurements and an extrapolation guided by a similarity method (Fig. 6b). Following Goutorbe et al. (2011), we stack different heat-flow proxies in order to get redundantinformation to better constrain the heat-flow predictions. The method is based on the evaluation, at each location of a grid (here, 0.1°x0.1°), of the number of similarities with several heat-flow proxies (called observables) at all other locations of the global grid where surface heat-flow is known. Observables used in Fig. 6b are from global geological and geophysical observations and models, as in the studies of Goutorbe et al. (2011) and Lucazeau (2019). To these global databases, we added information on the local geology of the Caribbean region (Fig. 6a). The heat-flow map we obtain is thus a predictive map. We retrieve the medium-scale features of surface heat-flow in the Caribbean that were described previously, with low heat-flow in the basins and higher heat-flow in the active Lesser Antilles Arc. For the Greater Antilles, the map emphasizes the overall cold thermal signature but also points out the existence of local-scale variability with high heat-flow along the northern faults of the Caribbean region.

4 Conclusions

New data for offshore Haiti show that background heat-flow, 40-50 mWm^{-2}, is consistent with older data from the Greater Antilles arc. However, high heat-flow was measured locally near

faults, in particular the E-W strike-slip SOFZ and small reverse faults south of it. Predictive heat-flow mapping suggests this is a pervasive feature along the strike of the SOFZ. Based on the analysis of the new data, we speculate that fluid circulation may be involved to produce such fault-related high heat-flow.

Away from the faults, heat-flow in the Greater Antilles falls to a regional heat-flow low. This uniformly low value across continental and oceanic domains is most probably related to a low radiogenic content of the continental crust. This low heat-flow pattern is confirmed at the scale of the Caribbean. Two exceptions are found in the tectonically active regions of the Lesser Antilles arc and Cayman trough. The new Caribbean heat-flow map shows that the only places that stand off to the low background heat-flow are the active zones of subduction, crustal accretion and large-scale transform faults.

Acknowledgments

We thank the crew of L'Atalante (IFREMER/GENAVIR) and the scientific team. We acknowledge constructive comments by two reviewers.

Data Availability

The data that support the findings of this study are available from the corresponding author upon reasonable request.

References

Anderson, R. N., Larue, D. K., 1991. Wellbore heat-flow from the Toa Baja scientific drillhole, Puerto Rico. Geophysical Research Letters 18, 537–540.

Berthier, F., Fabriol, R. & Puvillan, P., 1984. Evaluation des ressources géothermiques basse énergie en république d'Haïti, recherche d'un projet type – synthèse des travaux de terrain. Rapport B.R.G.M. 84 SGN 206 GTH.

Bookman, C. A., Malone, I., Langseth, M. G., 1972. Sea Floor Geothermal Measurements from Conrad Cruise 13. Tech. rep., Lamont-Doherty Geological Observatory Palisades N.Y.

Bookman, C. A., Malone, I., Langseth, M. G., 1973. Sea Floor Geothermal Measurements from Vema Cruise 26. Tech. Rep. 7-CU-7-73, Lamont-Doherty Geological Observatory Palisades N.Y.

Brune, J. N., Henyey, T. L., Roy, R. F., 1969. Heat-flow, stress, and rate of slip along the San Andreas fault, California. Journal of Geophysical Research 74, 3821–3827.

Calais, E., J. Perrot, and B. Mercier de Lépinay, 1998. Strike-slip tectonics and seismicity along the northern Caribbean plate boundary from Cuba to Hispaniola, in Active Strike-Slip and Collisional Tectonics of the Northern Caribbean Plate Boundary Zone, edited by J. F. Dolan and P. Mann, Geol. Soc. Am. Spec. Pap., 326.

Calais, E., S. Symithe, B. Mercier de Lépinay, and C. Prépetit, 2016. Plate boundary segmentation in the northeastern Caribbean from geodetic measurements and Neogene geological observations, Compt. Rendus Geosci., 348, 42–51, doi:10.1016/j.crte.2015.10.007.

Cermak, V., Kresl, M., Safanda, J., Bodri, L., Napoles-Pruna, M., Tenreyro-Perez, R., 1991. Terrestrial heat-flow in Cuba. Physics of the Earth and Planetary Interior 65, 207–209.

Cermak, V., Kresl, M., Safanda, J., Napoles-Pruna, M., Tenreyro-Perez, R., Torres-Paz, L. M., Valdes, J. J., 1984. First heat-flow density assessments in Cuba. Tectonophysics 103 (1–4), 283–296.

Clark, T. F., Korgen, B. J., Best, D. M., 1978. Heat-flow in the Eastern Caribbean. Journal of Geophysical Research 83 (B12), 5883–5891.

Corbeau, J., Rolandone, F., Leroy, S., de Lépinay, B. M., Meyer, B., Ellouz-Zimmermann, N., Momplaisir, R., 2016a. The northern Caribbean plate boundary in the Jamaica passage: Structure

and seismic stratigraphy. Tectonophysics 675, 209–226.

Corbeau, J., Rolandone, F., Leroy, S., Meyer, B., de Lépinay, B. M., Ellouz-Zimmermann, N., Momplaisir, R., 2016b. How transpressive is the northern Caribbean plate boundary? Tectonics 35 (4), 1032–1046.

Corbeau, J., Rolandone, F., Leroy, S., Guerrier, K., Keir, D., Stuart, G., Clouard, V., Gallacher, R., Ulysse, S., Boisson, D., Momplaisir, R., Preux, F. S., Prepetit, C., Saurel, J.-M., de Lépinay, B. M., Meyer, B., 2017. Crustal structure of western Hispaniola (Haiti) from a teleseismic receiver function study. Tectonophysics 709, 9–19.

Epp, D., Grim, P. J., Langseth, M. G., 1970. Heat-flow in the Caribbean and Gulf of Mexico. Journal of Geophysical Research 75, 5655–5669.

Erickson, A. J., Helsley, C. E., Simmons, G., 1972. Heat-flow and Continuous Seismic Profiles in the Cayman Trough and Yucatan Basin. Bulletin Geological Society of America 83, 1242–1260.

Fisher, A. T., Wheat, C. G., 2010. Seamounts as conduits for massive fluid, heat, and solute fluxes on ridge flanks. Oceanography 23.

Goutorbe, B., Poort, J., Lucazeau, F., and Raillard, S, 2011. Global heat-flow trends resolved from multiple geological and geophysical proxies, Geophysical Journal International, 187, 1405–1419, doi:10.1111/j.1365-246X.2011.05228.

Hayman, N.W., Grindlay, N.R., Perfit, M.R., Mann, P., Leroy, S., and de Lépinay, B.M., 2011. Oceanic core complex development at the ultraslow spreading Mid-Cayman Spreading Center. Geochemistry, Geophysics, Geosystems, 12 (3), 1–21.

Hutnak, M., Fisher, A., Stein, C., Harris, R., Wang, K., Silver, E., Spinelli, G., Pfender, M., Villinger, H., MacKnight, R., Costa Pisani, P., Deshon, H., Diamente, C., 2007. The thermal state of 18–24 ma upper lithosphere subducting below the nicoya peninsula, northern Costa Rica margin. In: MARGINS Theoretical Institute: SIEZE Volume. Columbia University Press, pp. 86–122.

Khutorskoy, M. D., Fernandez, R., Kononov, V. I., Polyak, B. G., Matveev, V. G., Rot, A. A., 1990.

Heat-Flow Through the Sea Bottom around the Yucatan Peninsula. Journal of Geophysical Research 95 (B2), 1223–1237.

Lachenbruch, A. H., Sass, J. H., 1992. Heat-flow from Cajon pass, fault strength, and tectonic implications. Journal of Geophysical Research 97 (B4), 4995–5015.

Langseth, M. G., Malone, I., Berger, D., 1971. Sea Floor Geothermal Measurements from VEMA Cruise 24. Tech. rep., Lamont-Doherty Geological Observatory Palisades N.Y.

Le Gal, V., F. Lucazeau, M. Cannat, J. Poort, C. Monnin, A. Battani, F. Fontaine, B. Goutorbe, F. Rolandone, C. Poitou, M-M. Blanc-Valleron, A.Piedade, A. Hipolito, 2018. Heat-flow, morphology, pore fluids and hydrothermal circulation in a typical mid-Atlantic ridge flank near Oceanographer Fracture Zone, Earth Planet. Sci. Lett.,482, doi:10.1016/j.epsl.2017.11.035.

Leroy S., Mauffret A., Patriat P. and Mercier de Lépinay B. 2000. An alternative interpretation of the Cayman trough evolution from a reindentification of magnetic anomalies - Geophys. J. Int., 141, 539-557.

Leroy, S., Ellouz-Zimmermann, N., Corbeau, J., Rolandone, F., Mercier de Lépinay, B., Meyer, B., Momplaisir, R., Granja Bruna, J. L., Battani, A., Baurion, C., Burov, E., Clouard, V., Deschamps, R., Gorini, C., Hamon, Y., Lafosse, M., Leonel, J., Le Pourhiet, L., Llanes, P., Loget, N., Lucazeau, F., Pillot, D., Poort, J., Tankoo, K. R., Cuevas, J., Alcaide, J. F., Jean Poix, C., Munoz-Martin, A., Mitton, S., Rodriguez, Y., Schmitz, J., Seeber, L., Carbo-Gorosabel, A., Munoz, S., 2015. Segmentation and kinematics of the north America-Caribbean plate boundary offshore Hispaniola. Terra Nova 27, 467–478.

Lewis, J. F., Kysar Mattietti, G., Perfit, M., Kamenov, G., 2011. Geochemistry and petrology of three granitoid rock cores from the Nicaraguan rise, Caribbean sea: implications for its composition, structure and tectonic evolution. Geologica Acta 9 (3-4), 467–479.

Lidiak, E.G., and Jolly, W.T., 1996: Circum-Caribbean Granitoids: Characteristics and Origin. International Geology Review, 38 (12), 1098–1133.

Loewen, M. W., Duncan, R. A., Kent, A. J. R., Krawl, K., 2013. Prolonged plume volcanism in the

caribbean large igneous province: New insights from curacao and Haiti. Geochemistry, Geophysics, Geosystems 14 (10), 4241–4259.

Lucazeau, F., 2019. Analysis and Mapping of an Updated Terrestrial Heat Flow Data Set. Geochemistry, Geophysics, Geosystems, 20, 4001-4024, doi: 10.1029/2019GC008389.

Manga, M., Hornbach, M. J., Le Friant, A., Ishizuka, O., Stroncik, N., Adachi, T., Aljah- dali, M., Boudon, G., Breitkreuz, C., Fraass, A., Fujinawa, A., Hatfield, R., Jutzeler, M., Kataoka, K., Lafuerza, S., Maeno, F., Martinez-Colon, M., McCanta, M., Morgan, S., Palmer, M. R., Saito, T., Slagle, A., Stinton, A. J., Subramanyam, K. S. V., Tamura, Y., Talling, P. J., Villemant, B., Wall-Palmer, D., Wang, F., 2012. Heat-flow in the Lesser Antilles island arc and adjacent back arc Grenada basin. Geochemistry Geophysics Geosystems 13, Q08007.

Mann, P., G. Draper, and J. F. Lewis,1991, An overview of the geologic and tectonic development of Hispaniola, Spec. Pap. Geol. Soc. Am., 262, 1–28, doi:10.1130/SPE262-p1.

Mase, C.W. and Smith, L., 1987. Effects of frictional heating on the thermal, hydrologic, and mechanical response of a fault, J. Geophys. Res., 92 (B7) (1987), pp. 6249-6272, 10.1029/JB092iB07p06249.

Mauffret A. & Leroy S., 1997. Seismic stratigraphy and structure of the Caribbean Igneous Province - Tectonophysics, 283, 61-104.

Nason, P. D., Lee, W. H. K., 1964. Heat-Flow Measurements in the North Atlantic, Caribbean and Mediterranean. Journal of Geophysical Research 69, 4875–4883.

Neill, I., Kerr, A.C., Hastie, A.R., Stanek, K.-P., and Millar, 2011. Origin of the Aves Ridge and Dutch– Venezuelan Antilles: interaction of the Cretaceous “Great Arc” and Caribbean–Colombian Oceanic Plateau ? Journal of the Geological Society, London, 168, 333–347.

Possee, D., Keir, D., Harmon, N., Rychert, C., Rolandone, F., Leroy, S., et al., 2019. The tectonics

and active faulting of Haiti from seismicity and tomography. Tectonics, 38. https://doi.org/10.1029/2018TC005364.

Rojas-Agramonte, Y., Neubauer, F., Kroner, A., Wan, Y. S., Liu, D. Y., Garcia-Delgado, D. E., Handler, R., 2004. Geochemistry and early palaeogene SHRIMP zircon ages for island arc granitoids of the Sierra Maestra, southeastern Cuba. Chemical Geology 213 (4), 307–324.

Rolandone F. and C. Jaupart, 2002. The distribution of slip rate and ductile deformation in a strike-slip shear zone, Geophys. J. Int., 148, 179-192.

Rosencrantz, E., Ross, M. I., Sclater, J. G., 1988. Age and Spreading History of the Cayman Trough as Determined from Depth, Heat-Flow, and Magnetic-Anomalies. Journal of Geophysical Research-Solid Earth and Planets 93, 2141–2157.

Sandwell, D., Schuber, G., 1982. Lithospheric flexure at fracture zones. Journal of Geo- physical Research 87 (B6), 4657–4667.

Vacquier, V., Von Herzen, R. P., 1964. Evidence for Connection Between Heat-flow and the Mid-Atlantic Ridge Magnetic Anomaly. Journal of Geophysical Research 69, 1093–1101.

Webber, A. P., Roberts, S., Murton, B. J., Hodgkinson, M. R. S., 2015. Geology, sulfide geochemistry and supercritical venting at the beebe hydrothermal vent field, Cayman trough. Geochemistry, Geophysics, Geosystems 16 (8), 2661–2678.

Webber, A. P., Roberts, S., Murton, B. J., Mills, R. A., Hodgkinson, M. R. S., 2017. The formation of gold-rich seafloor sulfide deposits: Evidence from the beebe hydrothermal vent field, Cayman trough. Geochemistry, Geophysics, Geosystems 18 (6), 2011–2027.

Figures captions

Figure 1: Bathymetric map of the Caribbean area with previous heat-flow measurements (colored dots) from the NGHF database (Lucazeau, 2019) and new measurements (colored stars) in the Haiti offshore. The main faults are shown. SOFZ: Septentrional-Oriente Fault Zone, EPGFZ: Enriquillo-Plantain-Garden Fault Zone, GB: Grenada Basin, LA: Lesser Antilles. The black square corresponds to the area of interest (Fig. 3).

Figure 2. Temperature-depth and thermal conductivity-depth profiles at each core location.

Figure 3. Heat-flow measurements offshore Haiti (except KT01 outside of the geographical area, see Fig. 1) with bathymetry. Cores measurements are represented by colored stars and BSR derived measurements by colored dots superimposed with seismic profiles acquired during HAITISIS in the Artibonite Basin. Heat-flow from 3 exploration drill-holes are shown with large colored dots with cross (Berthier et al., 1984, see Supplementary Material). Structural interpretations from Leroy et al. (2015) and Corbeau et al. (2016a,b) include the main strike-slip fault Septentrional-Oriente Fault Zone (SOFZ) in red and active reverse faults (black with triangles). The two seismic lines H12-118 and H12-103, shown in Fig. 4 and 5, are labeled.

Figure 4. Heat-flow estimated from BSR along seismic profile H12-118 (see localization in the inset). Upper panel: heat-flow vs shot number. The grey area displays the uncertainty on measurements (see explanations in the text). The closest heat-flow site from core KT16 is shown. Lower panel: time migrated seismic profile where arrows indicate the picked BSR.

Figure 5. Heat-flow estimated from BSR along seismic profile H12-103 (see localization in the inset). Upper panel: heat-flow vs shot number. The grey area displays the uncertainty on measurements (see Supplementary Material). Lower panel: time migrated seismic profile where arrows indicate the picked BSR.

Figure 6. a-Simplified map of distinct crustal domains in the Caribbean realm (de Lépinay, personal communication) with heat-flow measurements used in Fig.6b (colored dots). SOFZ:

Septentrional-Oriente Fault Zone, EPGFZ: Enriquillo-Plantain-Garden Fault Zone, GB: Grenada Basin, LA: Lesser Antilles. b- Heat-flow map based on similarities (see explanations in the text) with heat-flow measurements (colored dots). The high heat-flow measurements of Clark et al. (1978) in the Aves ridge are shown but not used (see text for discussion).

S.N.	Long.	Lat.	W.D.	nT	TG	nλ	λ	HF	S.HF
KT01	-75.274	17.8907	1524	2	78.28	9	1.08	84.81	15.05
KT04	-73.7492	18.8575	3569	5	54.58	12	0.89	48.71	6.21
KT05	-73.6610	18.7873	3276	5	41.72	13	1.01	42.26	2.62
KT06	-73.6058	18.8699	2161	5	46.13	10	0.99	45.67	3.54
KT07	-73.0691	18.5345	1549	5	43.87	11	0.92	40.36	1.65
KT08	-73.0173	18.5729	1692	5	38.39	9	0.92	35.19	1.24
KT10	-72.9992	18.5272	1630	5	51.34	11	0.88	45.18	3.10
KT12	-73.0209	20.1802	1700	4	82.85	10	1.07	88.98	5.90
KT13	-73.7018	19.972	3670	3	163.16	4	1.09	177.02	21.14
KT14	-73.1757	19.2607	1898	5	60.73	8	0.97	59.06	4.61
KT15	-73.3082	19.5357	1962	4	87.23	5	1.03	89.50	6.07
KT16	-73.3402	19.4906	1727	4	78.68	6	0.98	77.11	6.37

Table 1. Heat measurements: S.N.= site name; W.D.= water depth (m); nT = number of temperature determinations; T.G.= thermal gradient (mKm^{-1}); nλ = number of thermal conductivity determination; λ = thermal conductivity ($Wm^{-1}K^{-1}$); HF = Heat-flow (mWm^{-2}); S.HF= standard error on Heat-flow (mWm^{-2}).

Sites Names	Type of sedimentation	Type of crustal domain
KT01	Carbonate turbidites	Thinned island arc crust
KT04-05-06	Siliciclastic turbidites	Oceanic crust
KT07-08-10	Siliciclastic turbidites	Oceanic crust
KT12	Carbonate turbidites	Thinned island arc crust
KT13	Siliciclastic turbidites	Thinned island arc crust
KT14-15-16	Siliciclastic turbidites	Thinned island arc crust
Exploration drill-holes	Sandy-clayey detrital sediments	Cretaceous island arcs & oceanic terranes

Table 2. Type of sedimentation and crustal domain at the heat flow sites and at the drill-holes. The type of sedimentation is based on the sediment cores obtained during HAITI-SIS and from Berthier et al. (1984) for the exploration drill-holes. See Figure 6a for the type of crustal domain.

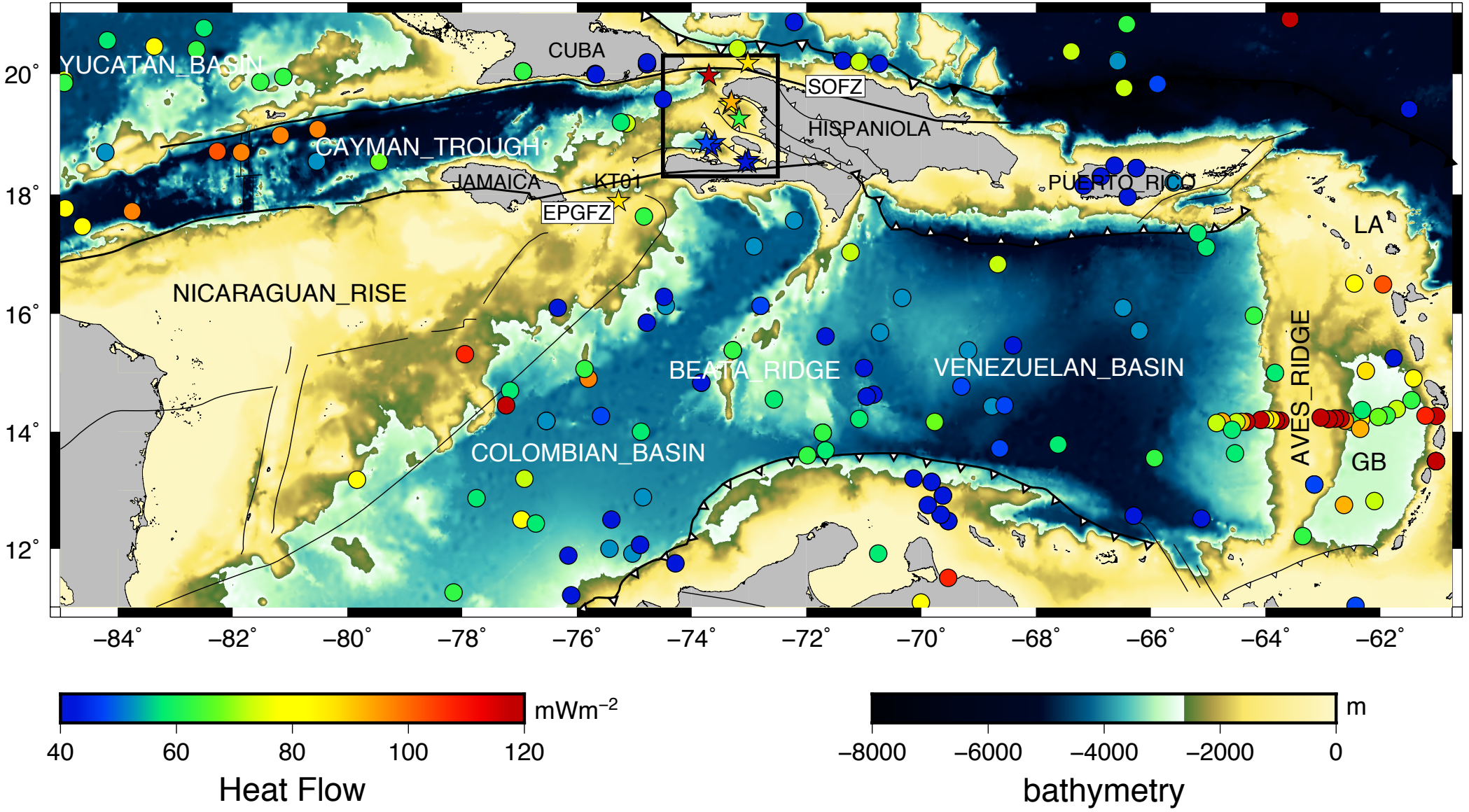
YUCATAN_BASIN
CUBA
SOFZ
HISPANIOLA
CAYMAN_TROUGH
JAMAICA
KT01
EPGFZ
PUERTO_RICO
LA
NICARAGUAN_RISE
BEATA_RIDGE
VENEZUELAN_BASIN
AVES_RIDGE
GB
COLOMBIAN_BASIN
20˚
18˚
16˚
14˚
12˚
−84˚
−82˚
−80˚
−78˚
−76˚
−74˚
−72˚
−70˚
−68˚
−66˚
−64˚
−62˚
mWm−2
40
60
80
100
120
Heat Flow
m
−8000
−6000
−4000
−2000
0
bathymetry

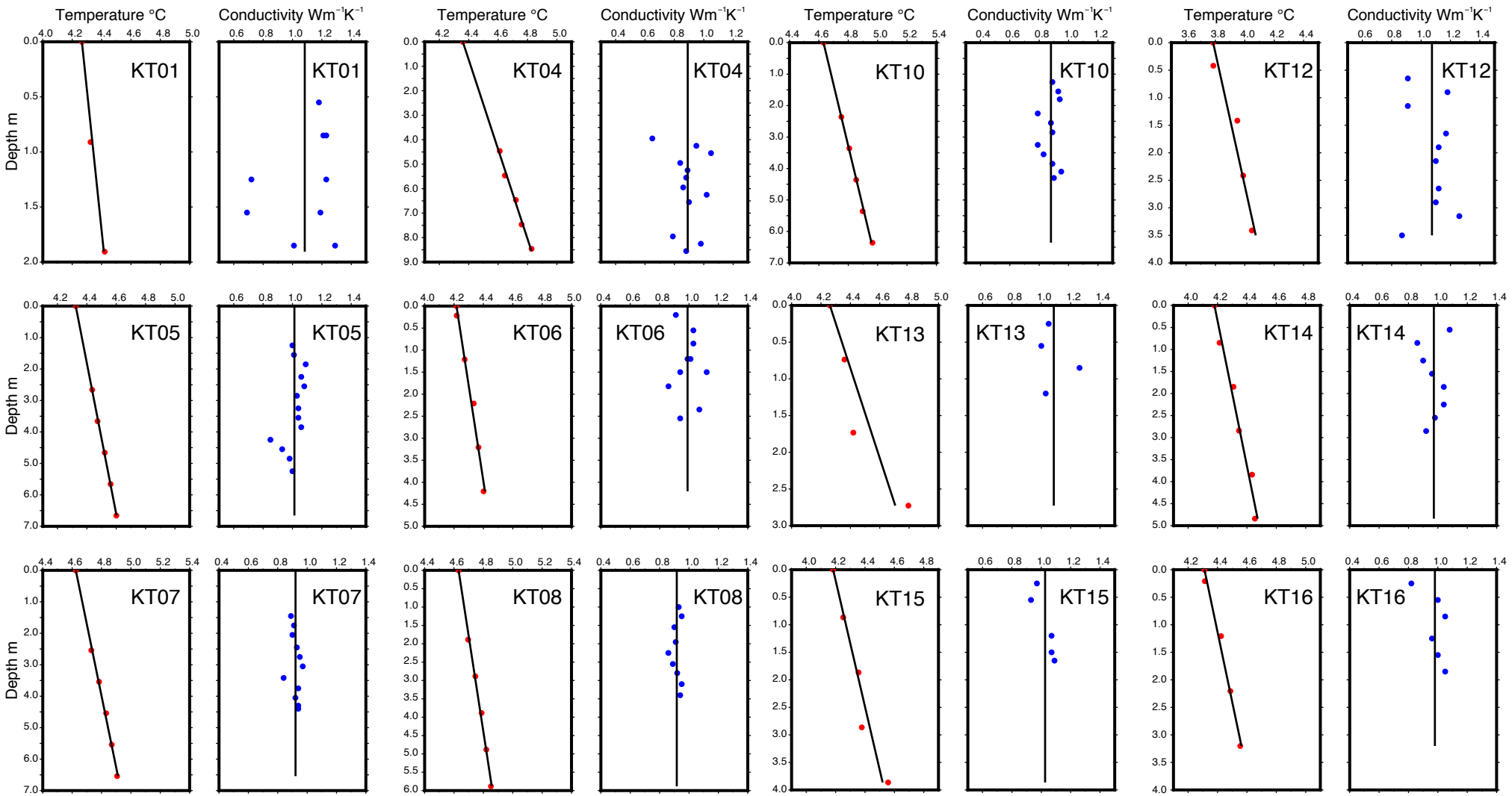
Temperature °C
Conductivity Wm⁻¹K⁻¹
Depth m
KT01
KT04
KT10
KT12
KT05
KT06
KT13
KT14
KT07
KT08
KT15
KT16

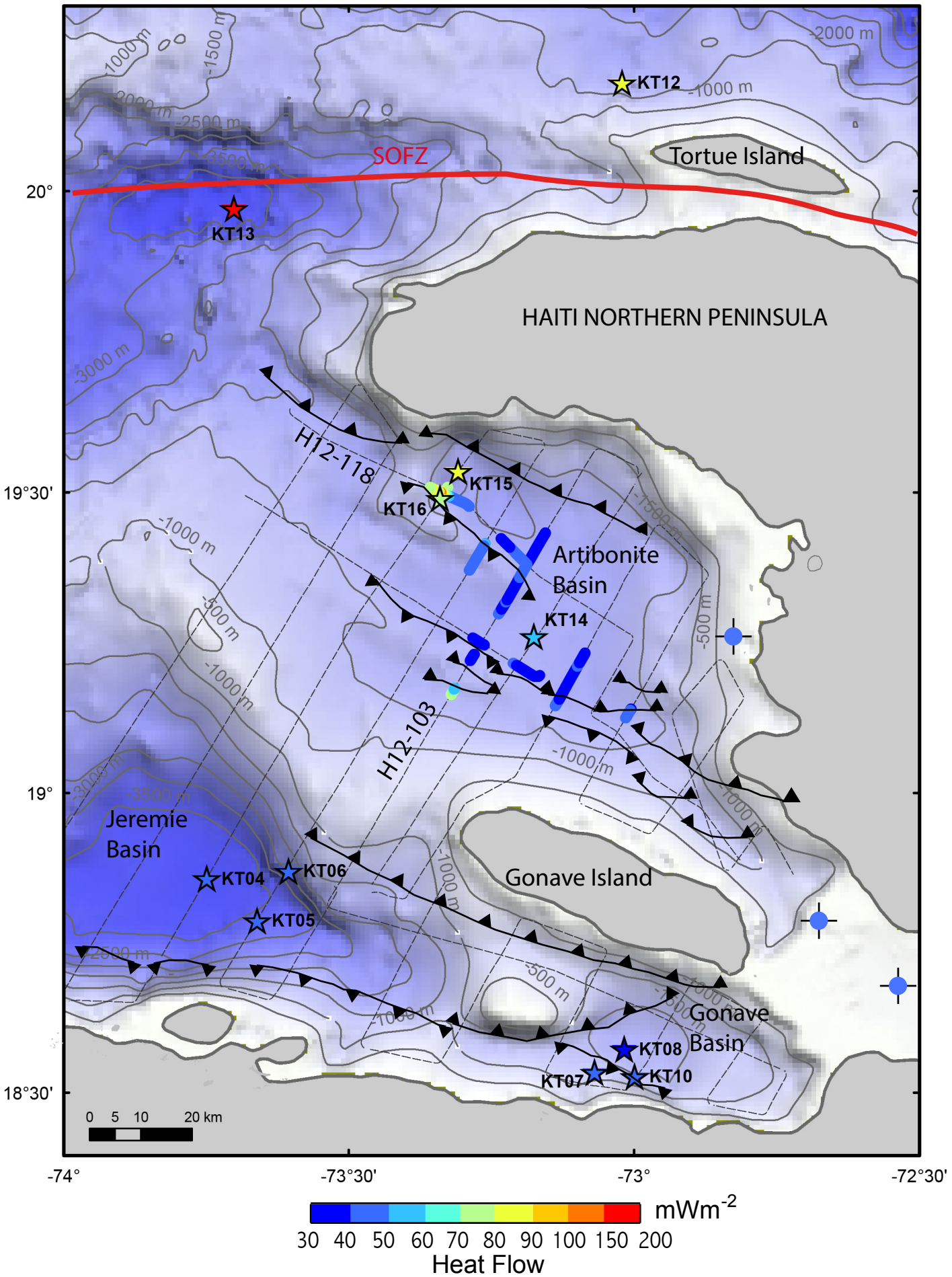
SOFZ
Tortue Island
HAITI NORTHERN PENINSULA
KT12
KT13
KT15
KT16
KT14
KT04
KT06
KT05
KT08
KT07
KT10
H12-118
H12-103
Artibonite Basin
Jeremie Basin
Gonave Island
Gonave Basin
-1000 m
-1500 m
-2000 m
-2500 m
-3000 m
-3500 m
-500 m
20°
19°30'
19°
18°30'
-74°
-73°30'
-73°
-72°30'
0 5 10 20 km
mWm-2
30 40 50 60 70 80 90 100 150 200
Heat Flow

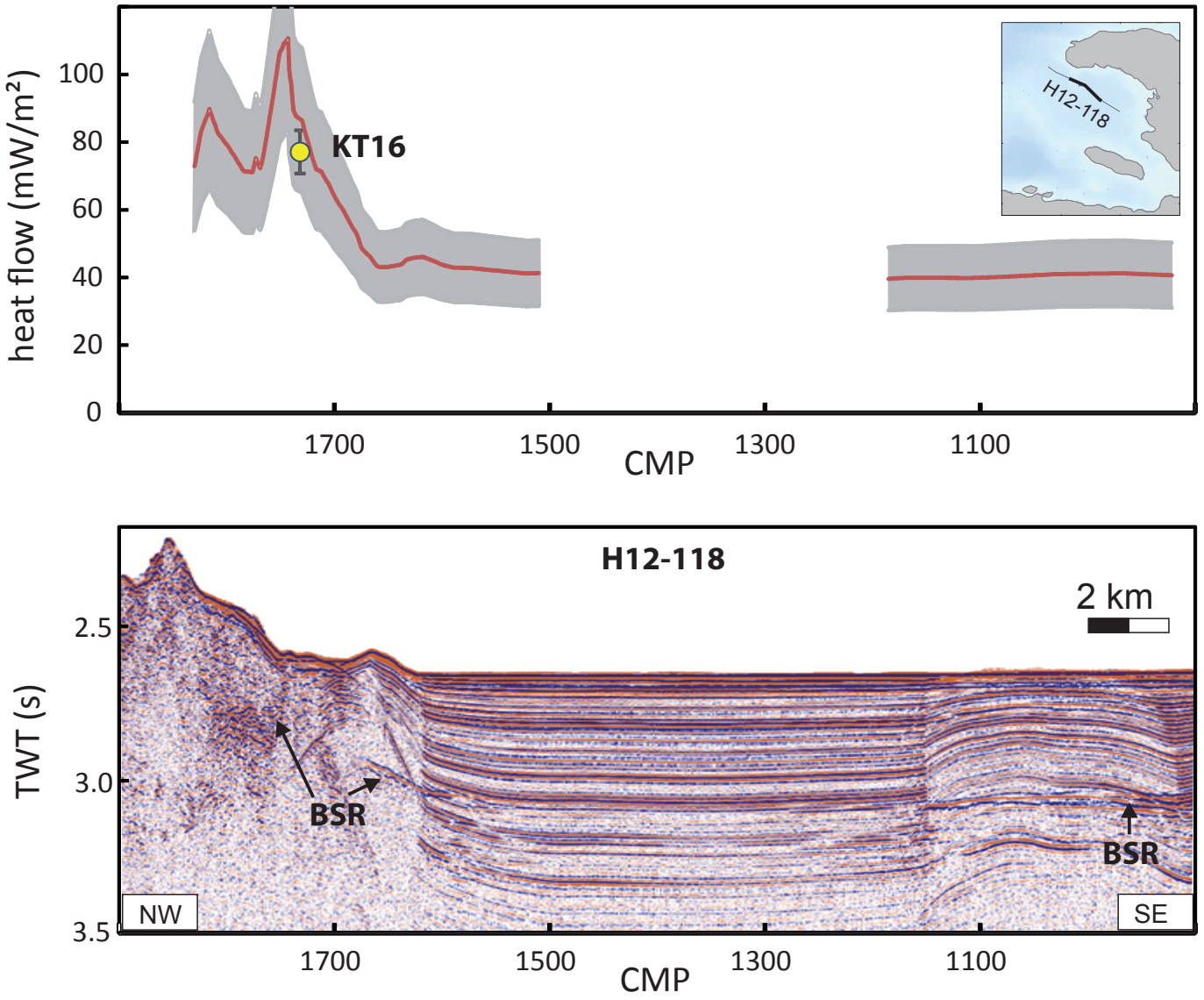
heat flow (mW/m²)
100
80
60
40
20
0
KT16
H12-118
1700
1500
1300
1100
CMP
H12-118
2 km
TWT (s)
2.5
3.0
3.5
BSR
BSR
NW
SE
1700
1500
1300
1100
CMP

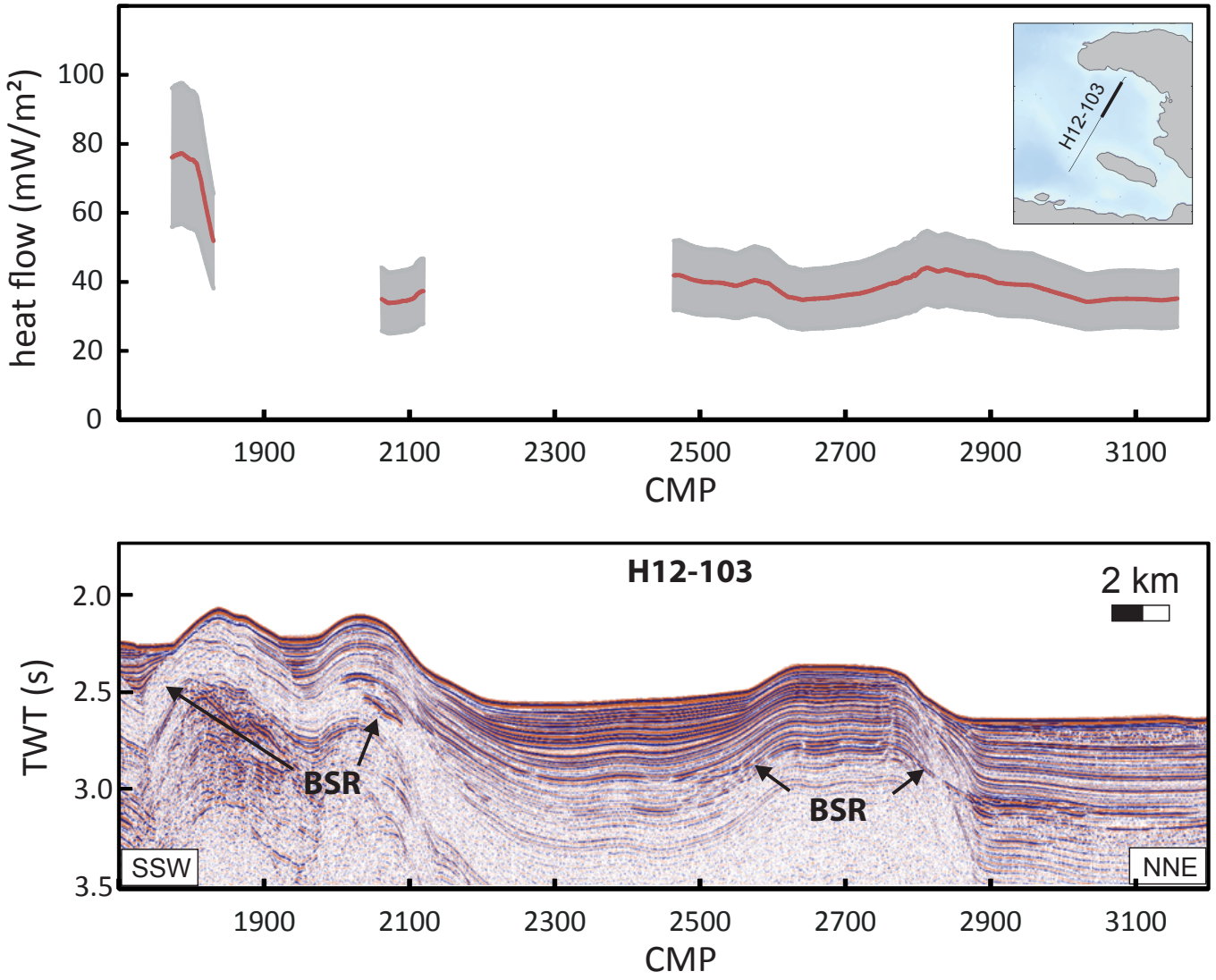
heat flow (mW/m²)
100
80
60
40
20
0
1900
2100
2300
2500
2700
2900
3100
CMP
H12-103
H12-103
2 km
TWT (s)
2.0
2.5
3.0
3.5
BSR
BSR
SSW
NNE
1900
2100
2300
2500
2700
2900
3100
CMP

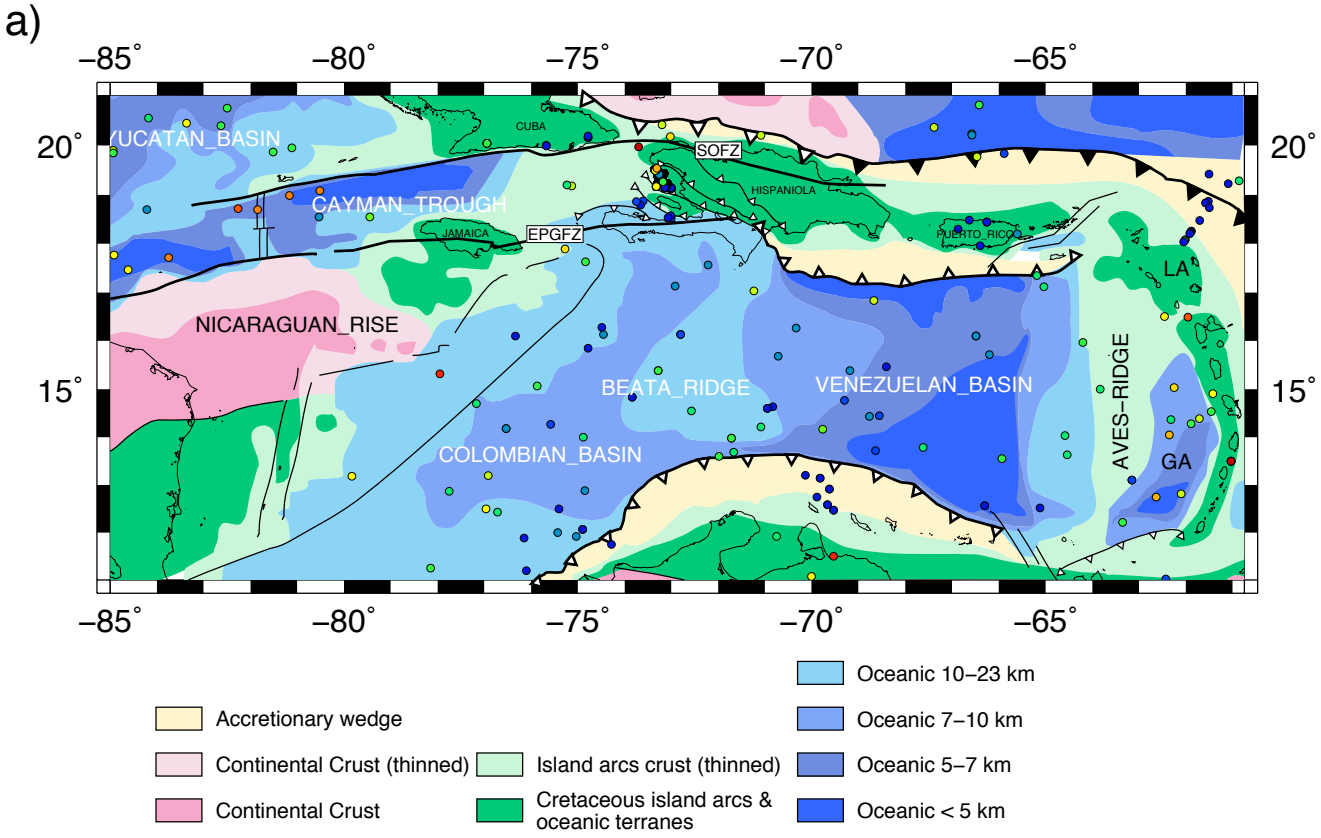
a)
−85˚
−80˚
−75˚
−70˚
−65˚
20˚
15˚
YUCATAN_BASIN
CUBA
SOFZ
CAYMAN_TROUGH
HISPANIOLA
JAMAICA
EPGFZ
PUERTO_RICO
LA
NICARAGUAN_RISE
BEATA_RIDGE
VENEZUELAN_BASIN
AVES−RIDGE
COLOMBIAN_BASIN
GA
Accretionary wedge
Continental Crust (thinned)
Continental Crust
Island arcs crust (thinned)
Cretaceous island arcs & oceanic terranes
Oceanic 10−23 km
Oceanic 7−10 km
Oceanic 5−7 km
Oceanic < 5 km

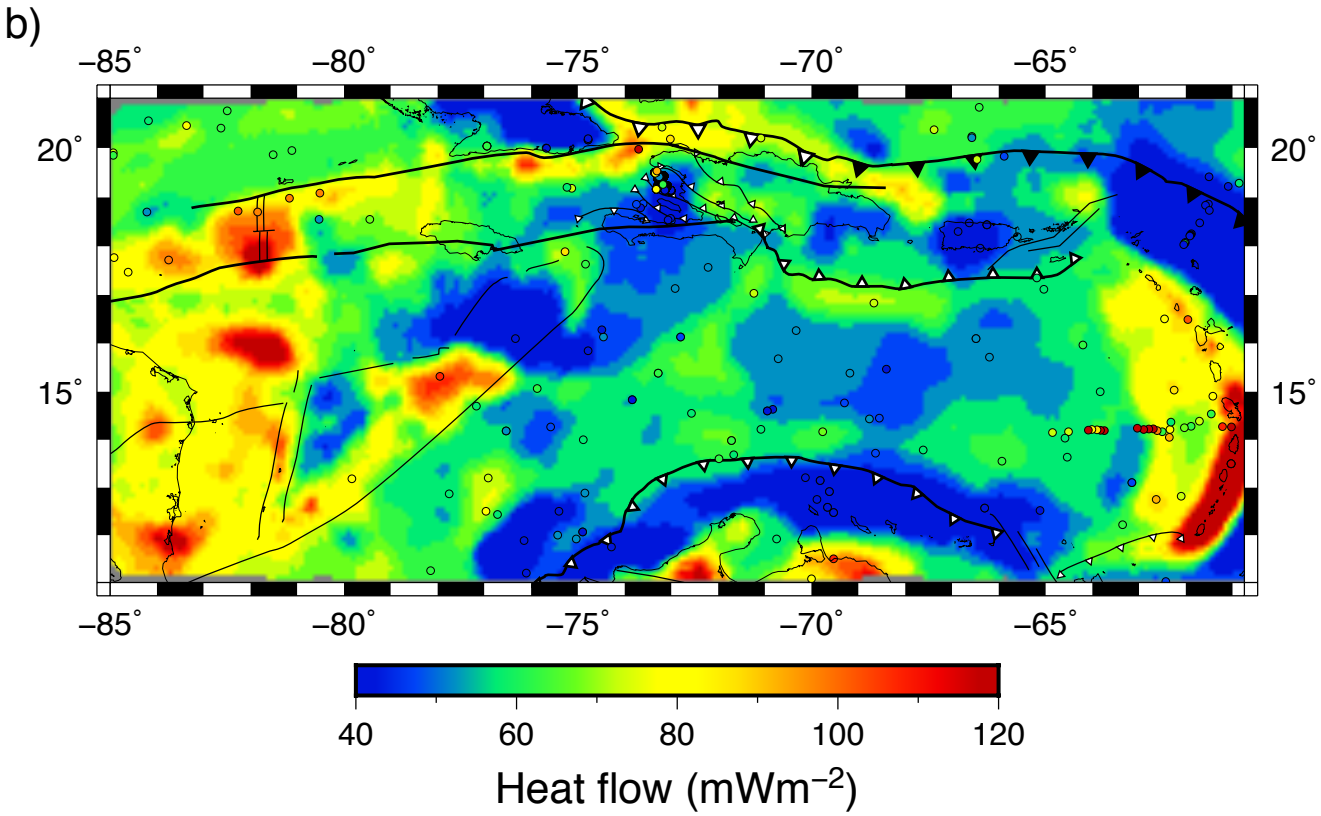
b)
−85˚
−80˚
−75˚
−70˚
−65˚
20˚
15˚
40
60
80
100
120
Heat flow (mWm−2)